Coupled-resonator optical waveguides for biochemical sensing of nanoliter volumes of analyte in the terahertz region

Hamza Kurt[a)] and D. S. Citrin
School of Electrical and Computer Engineering, Georgia Institute of Technology, Atlanta, Georgia 30332 and Georgia Tech Lorraine, 2-3 rue Marconi, Metz Technopole, 57070 Metz, France

(Received 4 February 2005; accepted 13 October 2005; published online 9 December 2005)

We present a detailed study of coupled-resonator optical waveguide (CROW) based sensors for biochemical sensing. The sensitivity dependence on the CROW structure parameters, such as intercavity distance and cavity type, is investigated for the effects in the THz region of the EM spectrum of introducing small quantities of molecules, such as DNA, in the holes. Introducing the absorptive material into the low-index medium greatly affects the shape of the propagating modes of the CROW and the transmitted E-field. The shift of the resonant frequency also depends linearly on the refractive index changes for off-resonant case (dispersive effect). © *2005 American Institute of Physics*. [DOI: 10.1063/1.2140479]

There are varieties of recently proposed biochemical sensors utilizing different configurations. For example, photonic crystal (PC) fiber (PCF) sensors based on the use of evanescent wave are the subject of considerable current research.[1,2] In general, the sensitivity of the evanescent-field sensor is low because exponentially decaying EM field penetrating to the sensing region is low. To increase the sensitivity one can use longer PCF, but then different issues have to be addressed such as increased sample quantities, greater latency, and the uniformly diffusion of the sample through the holes. Another example is the hollow-core antiresonant reflecting optical waveguides.[3] The hollow core is surrounded by high reflective Fabry-Pérot mirrors and can be filled with liquids to confine light and sense the analyte. Since light interacts only once as it propagates down the core, the sensitivity is low.

A number of these difficulties are potentially addressed by sensors based on PC cavities[4,5] and PC waveguides (PCW).[6] We have recently proposed PCW structures for biochemical sensing in the THz region.[7] The spectroscopic change in the transmission spectrum with the sample inserted into the holes in the line defect is monitored to ascertain the effect of the direct EM-matter interaction rather than the evanescent field-matter interaction as in PCF. The long effective pathlength over which the THz pulse interacts with the analyte was ensured without increasing the actual structure size by making sure that the propagating mode in the band gap has low group velocity (V_g). Moreover the field was confined largely within the holes where the sample is placed.

Recently, a new type of PCW called coupled-resonator optical waveguide (CROW) was introduced.[8] The waveguiding is based on tightly confining EM waves in each cavity and weakly coupling the cavities to their neighbors by the evanescent field of the resonator modes outside the cavity. Using the tight-binding approximation, it was shown that V_p and V_g strongly depend on the coupling parameter κ_1 which is controlled by cavity properties and intercavity distance.[9] Similar to the PCW, Vg of the propagating mode can be very low in CROW. On the other hand, CROWs have very sharp resonant propagating modes, which lead to enhanced field confinement compared with PCWs in which the modes are close to the band edge and confinement is poor. In this letter, we present the potential applications of CROW devices as biochemical sensor due to aforementioned properties.

We can briefly summarize our biochemical sensor design goals as follows. The first is to provide the interaction of the field with the target where the field is near its maximum, instead of via the evanescent part of the wave. In other words, the E-field maxima should be confined inside the holes where the analyte is loaded. This enhances the sensitivity. Second, we aim to increase the effective interaction length without making the structure larger. The advantages are twofold. Miniaturization is vital especially for integrated structures, and the ability to sense small quantities of analyte is of paramount importance for many biomedical applications. The selection of THz region of the EM spectrum brings the richness of the spectral features of many molecules with the ease of fabrication of PC based devices as well as the potential for real-time flow of fluids through the sensor for low-latency operation.

Below, the dispersive effect of the DNA molecules in CROWs is investigated by using finite-difference time-domain method with the recursive convolution approach.[10,11] The computational domain is terminated by a PML.[12] Each unit cell ($a\times a$) is divided into 30×30 grid points. CROWs are formed in 2D PC slabs with a triangular array of air holes in a GaAs dielectric background. We assume constant index of refraction $n=3.46$. The radius of the holes is $r=0.4a$ where a is the lattice periodicity and the schematic diagram is shown as an inset in Fig. 1(c). We use N and K to describe the number of air holes between each cavity and the number of cavities, respectively. For example in Figs. 1(a) and 1(b) $N=2$ and $K=5$. Cavities are created either increasing or reducing the radius of the holes to $r=0.45a$ and $r=0.3a$, respectively, and they are represented by CROW-A and -B. The defect free photonic crystal contains a band gap at $0.3504 < a/\lambda < 0.4176$ as shown in Fig. 1(c). We used the same parameters as in our previous work,[7] and uniform sample distribution is assumed. An aqueous solution of DNA sample may be delivered by injection, by free-fluid flow, or by integrated microfluidic channels onto the holes, and evaporation and desiccation carried out subsequently to ex-

a)Electronic mail: hkurt@ece.gatech.edu

0003-6951/2005/87(24)/241119/3/$22.50 © 2005 American Institute of Physics
Downloaded 24 May 2007 to 130.207.50.192. Redistribution subject to AIP license or copyright, see http://apl.aip.org/apl/copyright.jsp

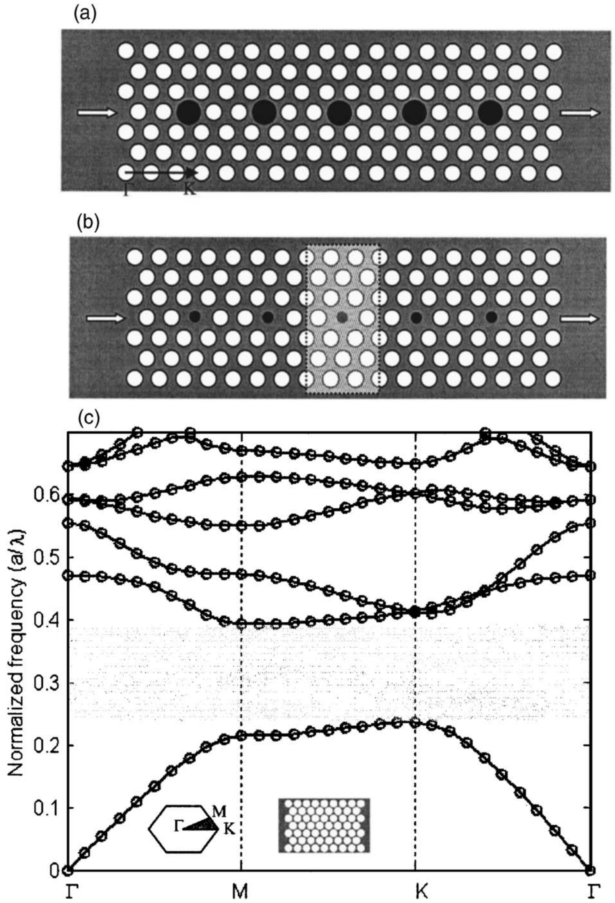

FIG. 1. (a) Schematic diagram of the CROW with increased air holes $r_{\text{def}}=0.45a$ (CROW-A). There are five defect cavities ($K=5$) and the number of holes between each cavity is 2 ($N=2$). (b) Schematic diagram of the CROW with the reduced holes $r_{\text{def}}=0.3a$ (CROW-B). N and K are the same as in (a). A supercell is highlighted. (c) Dispersion diagram of the unperturbed triangular array PC for TE mode.

clude THz absorption due to water. However, this may end up with a nonuniform sample distribution. Another way is to enable a loading process such that the sample distribution is uniform. For example, the filler can be obtained by mixing DNA with nonpolar liquids which are transparent and not strongly absorbing in the THz region. Another way is the immobilization of the biomolecule on the surfaces of the microchannels by covalently biding of the antibodies.[13]

Table I shows the different configurations studied here. $N=0$ means successive cavities occupy consecutive periods of the PC structure, resulting in the standard PCW. The resonant modes of CROWs are well inside the gap; hence, it is anticipated that the confinement of the E-field is strong.[14] The CROW structure can be interviewed as a chain of moderate Q cavities, N determining the Q. The E-field enhancement is proportional to Q. In effect, for a λ cavity, Q gives

TABLE I. Design parameters of the CROW operating in the THz region. The lattice periodicity is denoted by a and $a=60$ μm. Two types of defect radius were used $r_{\text{def}}=0.3a$ and $r_{\text{def}}=0.45a$. N and K describe the number of air holes between each cavity and the number of cavities, respectively.

N	K	r_{def}
1	7	$0.3a, 0.45a$
2	5	$0.3a, 0.45a$
3	3	$0.3a, 0.45a$

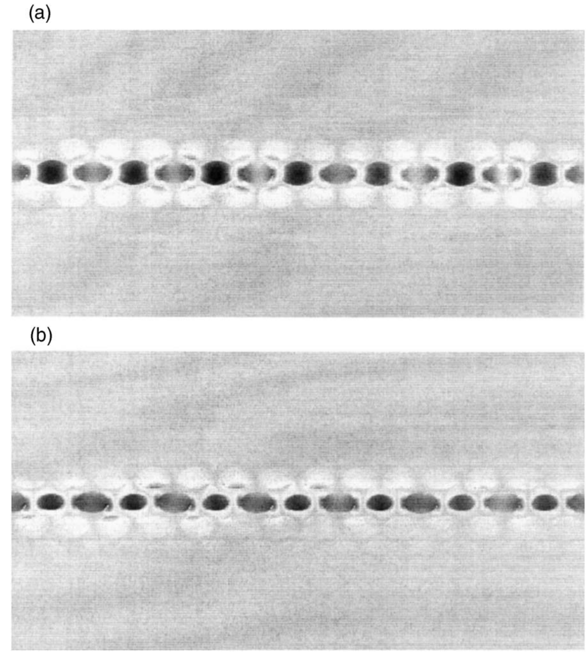

FIG. 2. (a) Steady-state E-field variation for CROW-A and (b) similarly for CROW-B with N equal to 1.

the number of times the E-field bounces around within the cavity before escaping. It can be seen, moreover, from Fig. 2 that E-field has large amplitude in defect sites with matching field maxima within the cavity where analyte is loaded.

It is important to note that as N increases V_g decreases. N has important effect to the overall transmission amplitude and also coupling of input light to the CROW. Increasing N reduces the transmitted light and also makes the coupling to the waveguide difficult; however, larger N means weak coupling between each cavity hence lower V_g. On the other hand, reducing N can increase the coupling factor and V_g. Thus, the judicious selection of N is important to ensure simultaneous low V_g and high transmission.

To compare the operation of the CROW sensor with either free-space cells or PCWs, it is essential to define the appropriate figure of merit. We defined the enhancement factor M (the details can be found in Ref. 7) as a measure of the change of attenuation induced by the CROW compared with bulk

$$M = \frac{z_1 \ln(E_{\text{out,CROW}}/E_{\text{in,CROW}})}{\Gamma z_2 \ln(E_{\text{out,bulk}}/E_{\text{in,bulk}})},$$

where Γ is the optical confinement factor measuring the degree of the concentration of the energy in sensing areas (i.e., holes), z_1 and z_2 measure the propagation distance within the gas cell or CROW. Figure 3 shows how M changes as N is increased. There is large improvement in M when N increases from 1 to 2, and even though the improvement in sensitivity continues to increase from $N=2$ to 3, the increase is not substantial. Therefore, $N=2$ can be selected considering a compact sensor structure. Also increasing $N>3$ may reduce the V_g and increase the sensitivity of the sensor but transmission amplitude at the output of the sensor will be small due to the difficulty in input coupling so that the detection will be difficult. Although CROW-A and -B exhibit similar trends in their M parameter, CROW-B has better performance than CROW-A because of the superior confine-

Downloaded 24 May 2007 to 130.207.50.192. Redistribution subject to AIP license or copyright, see http://apl.aip.org/apl/copyright.jsp

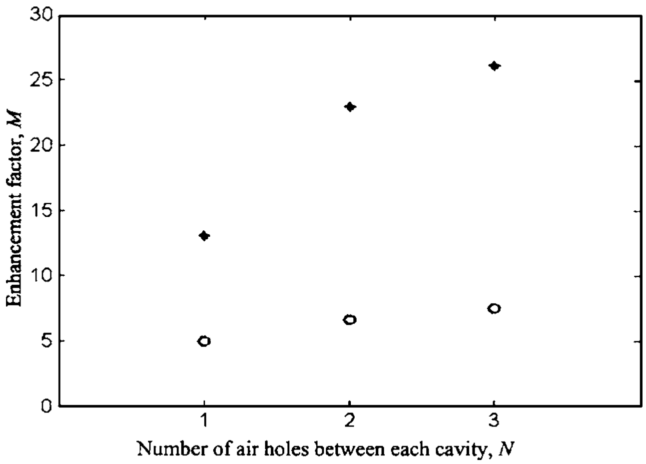

FIG. 3. The intercavity distance N vs enhancement parameter M for CROW-A (circle) and CROW-B (plus).

ment of the field modes; however, structures of the type of CROW-A may be desirable for practical reasons due to the larger air holes, and the consequent relative ease of loading the sample.

The other crucial parameter is K that comprises the CROW. The transmitted field shows exponential dependence on the length of the CROW. Longer waveguides, however, may increase the response time which may not be desired especially for real-time sensing. Also, sensor size is of paramount importance for integrated devices. Another issue in some applications is the ability to sense small quantities of material. Therefore selection an optimum value of K is important.

Figures 4(a) and 4(b) show the variation of resonant frequency when index of the analyte changes from $n=1.414$ to $n=1.581$. The spectral peak experiences redshift for both CROW-A and B as the index increases. The shift in CROW-A, however, is more than two times larger than in B, as can be seen in Fig. 4(c). One sees a linear relation between the frequency and the refractive index. As the index increases the propagating mode moves away from the air band. An index change of $\Delta n=0.033$ corresponds to a wavelength shift of $\Delta\lambda=1.17$ μm. It is also interesting to note that since both CROW-A and B have propagating mode pulled down from air band they show similar variation to the refractive index change.

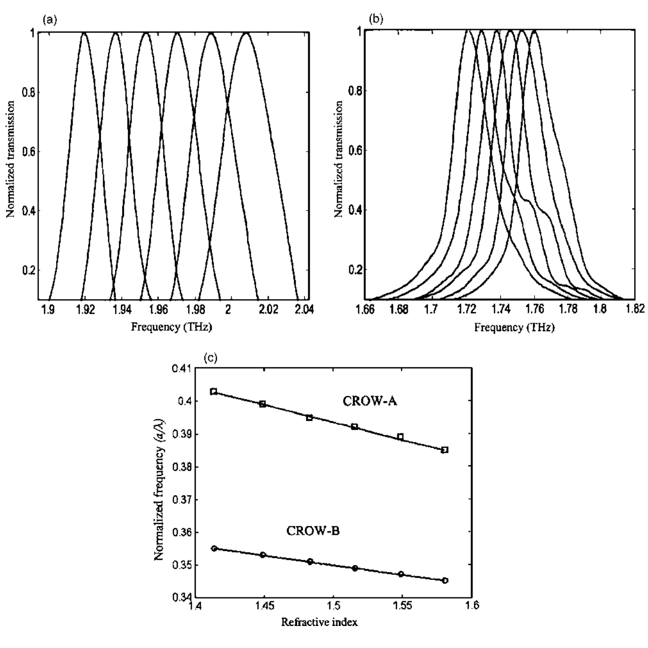

FIG. 4. (a) Resonant frequency shift of CROW-A for six different cases ($n=1.414$ to $n=1.581$). (b) Similarly for CROW-B. (c) Normalized frequency variation for the same refractive indexes.

The absorptive medium greatly changes the spectral shape of the resonant mode both in amplitude and width for on and off-resonance cases. Amplitude and width increase as the center frequency of the Lorentz medium moves away from that of the resonant mode. The Q of the resonant mode is modified. As the absorption peak of the analyte and the resonant mode of the waveguide overlap the change in the transmission spectrum is large compared to the off-resonant case. As a result this is a more sensitive detection regime.

In conclusion, after carrying out detailed simulations we have shown that very high sensitive biochemical sensors can be designed by selecting appropriately the CROW parameters (defect radius, number of cavities, and intercavity distance) in the THz. If the sample has weak absorbance then CROW-B type of structure is favorable due to high M factor. On the other hand, CROW-A is more sensitive simply because of more material used. The sensor is extremely sensitive to the changes in the absorption of the nanoliter volume samples. We have shown that the enhancement, M, of CROW-based sensors may be much higher than bulk structure and PCWs. We have attributed the better enhancement and sensitivity of the proposed sensor to the low V_g hence longer field-matter interaction, and the strong confinement of the field maxima in the low index medium where the analyte is loaded. Integration of such sensors with microfluidics may enable high-throughput, real-time THz sensors. The idea proposed in this work can be applied directly to the mid-infrared too.

This material is based upon work supported in part by the National Science Foundation under Grant No. 0305524.

[1] Y. L. Hoo, W. Jin, C. Shi, H. L. Ho, D. N. Wang, and S. C. Ruan, Appl. Opt. **42**, 3509 (2003).
[2] J. B. Jensen, L H. Pedersen, P. E. Hoiby, L. B. Nielsen, T. P. Hansen, J. R. Folkenberg, J. Riishede, D. Noordegraaf, K. Nielsen, A. Carlse, and A. Bjarklev, Opt. Lett. **29**, 1974 (2004).
[3] D. Yin, D. W. Deamer, H. Schmidt, J. P. Barber, and A. R. Hawkins, Appl. Phys. Lett. **85**, 3477 (2004).
[4] M. Loncar, A. Scherer, and Y. Qiu, Appl. Phys. Lett. **82**, 4648 (2003).
[5] E. Chow, A. Grot, L. W. Mirkarimi, M. Sigalas, and G. Girolami, Opt. Lett. **29**, 1093 (2004).
[6] J. Topol'ancik, P. Bhattacharya, J. Sabarinathan, and P.-C. Yu, Appl. Phys. Lett. **82**, 1143 (2003).
[7] H. Kurt and D. S. Citrin, Appl. Phys. Lett. **87**, 41108 (2005).
[8] A. Yariv, Y. Xu, R. K. Lee, and A. Scherer, Opt. Lett. **24**, 711 (1999).
[9] M. Bayindir, B. Temelkuran, and E. Ozbay, Phys. Rev. Lett. **84**, 2140 (2000).
[10] A. Taflove, *Computational Electrodynamics, The Finite-Difference Time-Domain Method* (Artech House, Boston, 1995).
[11] K. S. Kunz, *The Finite Difference Time Domain Method for Electromagnetics* (CRC, Boca Raton, FL, 1993).
[12] J. P. Berenger, J. Comput. Phys. **114**, 185 (1994).
[13] Z. L. Zhang, C. Crozaiter, M. Le Berre, and Y. Chen, Microelectron. Eng. **78–79**, 556, (2005).
[14] Y. Xu, R. K. Lee, and A. Yariv, J. Opt. Soc. Am. B **17**, 387 (2000).

Downloaded 24 May 2007 to 130.207.50.192. Redistribution subject to AIP license or copyright, see http://apl.aip.org/apl/copyright.jsp